Carcinogenesis vol.32 no.5 pp.723–731, 2011
doi:10.1093/carcin/bgr038
Advance Access publication February 28, 2011

Lipid raft-dependent death receptor 5 (DR5) expression and activation are critical for ursodeoxycholic acid-induced apoptosis in gastric cancer cells

Sung-Chul Lim[1,2,†], Hong-Quan Duong[1,†], Jeong Eun Choi[1], Tae-Bum Lee[1], Ju-Hee Kang[3], Seung Hyun Oh[3] and Song Iy Han[1,*]

[1]Research Center for Resistant Cells and [2]Department of Pathology, Chosun University, Gwangju 501-759, Korea and [3]Research Institute National Cancer Center, Goyang-si, Gyeonggi-do 410-769, Korea

*To whom correspondence should be addressed. Tel: +82 62 233 6053; Fax: +82 62 233 6052;
Email: sihan@chosun.ac.kr

Ursodeoxycholic acid (UDCA) is known as a suppressor of cholestatic liver diseases and colorectal cancer development. Here, we demonstrate that UDCA induces apoptosis without necrotic features in SNU601, SNU638, SNU1 and SNU216 human gastric cancer cells, implying its possible use as an effective chemotherapeutic agent in treatment of gastric cancer. UDCA-induced apoptosis was dominantly mediated by an extrinsic pathway dependent on caspase-8, -6 and -3. UDCA increased expression of death receptor 5 [(DR5), also known as tumor necrosis factor-related apoptosis-inducing ligand (TRAIL) receptor 2], and this DR appeared to be responsible for UDCA-induced apoptosis, as evidenced by DR5 knockdown. UDCA triggered formation of lipid rafts that played crucial roles in UDCA-induced apoptotic actions. Lipid rafts were required not only for provision of a proper site for DR5 action but also for mediation of DR5 expression. In addition, reactive oxygen species (ROS) and protein kinase C (PKC) δ appeared to be implicated in UDCA-induced raft-dependent DR5 expression. Our results indicate that UDCA-induced apoptosis is mediated by DR5 expression, which is regulated by the raft formation/ROS production/PKCδ activation pathway and DR5 localization into lipid rafts in gastric cancer cells. Tumor-suppressive activity of UDCA was confirmed in an *in vivo* system: UDCA (120 mg/kg/day) significantly decreased tumor growth in gastric cancer xenograft mice. Taken together, our results demonstrate that UDCA can be used as a potent chemotherapeutic agent for treatment of gastric cancer.

Among various types of cancer, gastric carcinoma (GC) is one of the leading causes of cancer-related death worldwide, despite development of various surgical and chemotherapeutic treatments (1). Currently, surgical resection is the mainstay of treatment; however, many GC cases are diagnosed at advanced stages. Therefore, chemotherapy, combined with surgery, is another important option for treatment of unresectable cancers or for improvement of the prognosis. Indeed, platinum-fluoropyrimidine and cisplatin/capecitabine have been shown to promote the survival rate of advanced GC patients (2). However, the median overall survival is no >12 months, and the main obstacles of chemotherapy may be toxic side-effects; hence, new therapeutic strategies involving non-toxic compounds are worthy of development.

Abbreviations: DCA, deoxycholic acid; DCFDA, 2′,7′-dichlorofluorescin diacetate; DR, death receptor; DISC, death-inducing signaling complex; FADD, Fas-associated death domain; FITC, fluorescein isothiocyanate; FLICE, FADD-like IL-1β-converting enzyme; HEPES, *N*-2-hydroxyethylpiperazine-*N*′-2-ethanesulfonic acid; GC, gastric carcinoma; HO, Hoechst 33342; LDH, lactate dehydrogenase; MBCD, methyl-beta-cyclodextrin; MTT, 3-(4, 5-dimethylthiazol-2-yl)-2, 5-diphenyltetrazolium bromide; NAC, N-acetyl-L-cysteine; NADPH, reduced nicotinamide adenine dinucleotide phosphate; PARP, poly(ADP-ribose) polymerase; PKC, protein kinase C; ROS, reactive oxygen species; siRNA, small interference RNA; TRAIL, tumor necrosis factor-related apoptosis-inducing ligand; UDCA, ursodeoxycholic acid.

[†]These authors contributed equally to this work.

Ursodeoxycholic acid (UDCA) is a hydrophilic bile acid, which in humans only accounts for 4% of total bile acid. Unlike toxic hydrophobic bile acid, which acts as a carcinogen in various organs, including liver, colon and gastrointestine, hydrophilic bile acid has been constantly suggested as a tumor suppressor of hepatocellular carcinoma and colon cancer, as well as a reducer of cholestatic liver diseases (3–6). Although the tumor-suppressive activity of UDCA seems to be linked to its inhibitory effect on oncogenic factors in the colon (7), the mechanism underlying the antitumor effects of UDCA is not fully understood. Toxic bile acids due to duodenogastric reflux in the gastrointestine have been implicated in cancer development; UDCA prevents toxic bile acid-induced gastric cytotoxicity and gastritis (8,9). Therefore, the antitumor role of UDCA in GC cells has been suggested; however, this has not been investigated.

Apoptosis and necrosis, two types of cell death modes, may have different effects on pathophysiology (10,11). Necrosis is known to promote tumor progression by release of proinflammatory cytokine high mobility group box 1, due to membrane rupture, whereas, apoptosis is a tumor-suppressive type of cell death with limited inflammation. Apoptosis is mainly regulated by two pathways: a death receptor (DR)-mediated extrinsic pathway involving caspase-8 activation and a mitochondria-linked intrinsic pathway that includes caspase-9 activation. DRs are members of the tumor necrosis factor receptor superfamily, including CD95/Fas, tumor necrosis factor-related apoptosis-inducing ligand receptors (TRAIL-R/DR) and tumor necrosis factor related-I (12). Fas and TRAIL-R/DR are activated when they are engaged by association with their respective ligands, FasL and TRAIL; however, these DRs can also be activated in a ligand-independent fashion. Due to its selective ability for killing of tumor cells with little effect on normal cells, the TRAIL pathway has emerged as an attractive target for cancer therapy (13). Among the five different identified receptors that bind to TRAIL, only two, TRAIL-R1 (DR4) and TRAIL-R2 (DR5), contain a cytoplasmic death domain and trigger apoptosis, whereas the others (TRAIL-R3, TRAIL-R4 and osteoprotegerin) are decoy receptors. Upon activation, DRs form death-inducing signaling complexes (DISCs) that consist of receptors, Fas-associated death domains (FADD) and initiator caspase-8, resulting in activation of downstream caspases, with or without mitochondrial amplification of the signal (14). Functional activity of DRs, such as Fas, tumor necrosis factor related and DR5, requires their physical association with lipid rafts, which serve as plasma membrane platforms for DR-initiated signals in formation of efficient DISCs (15,16). Lipid rafts are dynamic, tightly ordered microdomains of the plasma membrane with various shapes and sizes and are highly enriched in cholesterol, sphingolipids and gangliosides (17). Since they play a critical role in various cellular events, including endocytosis, vesicle trafficking and cell death, lipid rafts have been suggested as a target for new strategies for control of cell death.

In this study, we examined the possible chemotherapeutic activity of UDCA in GC cells. We demonstrate that UDCA induces apoptosis without necrotic features in human gastric cancer cells and that UDCA-induced apoptosis is mediated by DR5 expression, which is regulated by the raft formation/reactive oxygen species (ROS) production/protein kinase C (PKC) δ activation pathway and DR5 localization into lipid rafts, indicating that UDCA can be used as a potent chemotherapeutic agent for treatment of gastric cancer.

Materials and methods

Cell culture and drug treatment

SNU601, SNU638, SNU1 and SNU216 human GC cell lines, which were obtained from the Korea Cell Line Bank, were grown in RPMI 1640 medium (Invitrogen, Carlsbad, CA) supplemented with 10% (vol/vol) fetal bovine serum and 1% antibiotics at 37°C in 5% CO_2. UDCA was purchased from ICN

Biomedicals (Irvine, CA) and unless specified, other drugs were purchased from Calbiochem (San Diego, CA).

Hoechst 33342/propidium iodide double staining

Treated cells were stained with an Hoechst 33342 (HO)/propidium iodide mixture and observed under a fluorescence microscope (DM5000, Leica, Wetzlar, Germany), as described elsewhere (18). A total of 500 cells from randomly chosen fields were counted and the number of apoptotic cells was expressed as a percentage of the total number of cells counted.

Lactate dehydrogenase (LDH) release and 3-(4, 5-dimethylthiazol-2-yl)-2, 5-diphenyltetrazolium bromide (MTT) viability assays were performed.

According to the manufacturer's protocol, LDH release was quantified using the LDH cytotoxicity assay kit II (BioVision, Mountain View, CA) (18). The percentage of specific-LDH release was calculated by the following formula: % cytotoxicity = [(experimental LDH release) − (spontaneous LDH release by effector and target)/(maximum LDH release) − (spontaneous LDH release)] × 100. For the MTT assay, cells were incubated with MTT solution (0.5 mg/ml) and solubilized using dimethylsulfoxide, and the solubilized formazan product was quantified as absorbance at 595 nm, as described elsewhere (18).

Clonogenic assay

Cells treated with UDCA for 12 h were trypsinized, washed and replated (2000 cells/60 mm dish). Following incubation for 14 days in a 37°C/5% CO_2 incubator, colonies were stained using crystal violet and scored (>1 mm).

Immunoblotting

Using a standard technique, equal amounts of protein were electrophoretically separated using sodium dodecyl sulfate–polyacrylamide gel electrophoresis and transferred to a nitrocellulose membrane. Antibodies were used to probe for active caspase-6, active caspase-3 (Cell Signaling Technology, Danvers, MA), poly(ADP-ribose) polymerase (PARP), Fas, FADD, caveolin-1 (Santa Cruz Biotechnology, Santa Cruz, CA), DR4, DR5 (ProSci Inc., Poway, CA), RIP1, PKCα, PKCδ, PKCε and PKCθ (BD sciences, San Diego, CA). Anti-α-tubulin (BioGenex Laboratories, San Ramon, CA) was used as a loading control. An image analyzer (Image Station 4000MM; Kodak, Carestream Health Inc., Rochester, NY) was used for acquisition of signals.

Caspase-8 activity assay

According to the manufacturer's protocol, a FADD-like IL-1β-converting enzyme (FLICE) colorimetric assay kit (BioVision) was used for performance of the caspase-8 activity assay. Briefly, 200 μg protein lysates in a 50 μl volume was mixed with reaction buffer, mixed with IETD-p-nitroanilide substrate, incubated for 90 min, and absorbance was measured at 405 nm. Fold increase in FLICE activity was determined by comparison of the results of treated samples with the level of the untreated control.

Real-time reverse transcription–polymerase chain reaction

Real-time polymerase chain reaction was performed with the Light Cycler 2.0 (La Roche, Fribourg, Switzerland) using the Fast Start DNA Master SYBR Green I Kit (Roche). For verification of the correct amplification product, polymerase chain reaction products were analyzed on a 2% agarose gel stained with ethidium bromide. Primer sequences were as follows: for β-actin, 5′- for Fas; 5′-TGGCACGGAACACACCCTGAGG-3′ and 5′-GAGGGTCCAGATGCCCAG-CATG-3, for DR5; 5′-GCCTCATGGACAATGAGATAAGGTGGCT-3′ and 5′-CCAAATCTCAAAGTACGCACAAACGG-3, for DR4; 5′-ATGGCGCCAC-CACCAGCTAGAG-3′ and 5′-CCCGCCTCGTGGTTCAATCCTC-3 and for TRAIL, 5′-ATGGCTATGATGGAGGTCCAG-3′ and 5′-TTGTCCT-GCATCTGCTTCAGC-3′. Melting curve analysis was performed to confirm production of a single product. Negative controls without template were produced for each run. Data were analyzed using Light Cycler software version 4.0 (Roche).

RNA interference

For the RNA interference experiment, small interference RNA (siRNA) of DR5, 5′- CAGACUUGGUGCCCUUUG (dtdt)-3′ (sense strand (S)) and 5′-UCAAAGGGCACCAAGUCUG (dtdt)-3′ (antisense strand (AS)), PKCδ 5′-CU-CAUGGUACUUCCUCUGU (dtdt)-3′ (S) and 5′-ACAGAGGAAGUACCAU-GAG (dtdt)-3′ (AS), RIP1, 5′-CACACAGUCUCAGAUUGAU (dtdt)-3′ (S) and 5′-AUCAAUCUGAGACUGUGUG (dtdt)-3′ (AS) and FADD, 5′-CCAAGAUC-GACAGCAUCGA (dtdt)-3′ (S) and 5′-UCGAUGCUGUCGAUCUUGG (dtdt)-3′ (AS) and control siRNA, 5′-CCUACGCCACCAAUUUCGU (dtdt)-3′ (S) and 5′-ACGAAAUUGGUGGCGUAGG (dtdt)-3′ (AS) were purchased from BION-EER (Daejeon, Korea). Using the Amaxa transfection kit, a total of 10^6 cells were transfected with 8 μg siRNA, and cells were then grown for 24 h prior to treatment.

Lipid raft fractionation

Lipid rafts were isolated using sucrose density-gradient centrifugation. A total of 10^8 cells were lysed for 30 min in 1 ml lysis buffer [1% Brij35 in *N*-2-hydroxyethylpiperazine-*N*′-2-ethanesulfonic acid (HEPES) buffer; 25 mM HEPES, 1 mM ethylenediaminetetraacetic acid and 150 mM NaCl, pH 6.5] supplemented with a protease inhibitor cocktail and homogenized with a glass Dounce homogenizer. Homogenates were mixed with 1 ml of 80% sucrose in HEPES buffer and placed at the bottom of a centrifuge tube. Samples were then overlaid with 6.5 ml of 30% sucrose and 3 ml of 5% sucrose and centrifuged at 188 000*g* for 18 h at 4°C. Fractions (1 ml) were collected from the bottom to the top of the gradient, then precipitated and subsequently analyzed using immunoblotting.

Isolation of membrane proteins

According to the manufacturer's protocol, cells were fractionated into cytosol and membrane fractions using a Subcellular ProteoExtract® Kit (Calbiochem). Anti-caveolin-1 was used as a marker of membranous protein.

Assays for ROS

For measurement of ROS generation, cells were treated with UDCA for the indicated times and loaded with 50 μM 2′,7′-dichlorofluorescin diacetate (DCFDA; Molecular Probes, Eugene, OR) and 0.5 μg/ml HO for 30 min. After rinsing, fluorescent images were taken with an inverted fluorescence microscope or fluorescence intensities were obtained with a Fluorocount (Perkin Elmer) at excitation/emission wavelengths of 490/530 nm (DCFDA) and 340/425 (HO), and values of ROS production were obtained by determining the ratio of DCFDA/HO signals per well.

Confocal microscopy

Cells grown on coverslips were fixed with 1.5% paraformaldehyde for 10 min at −20°C and then blocked for 1 h at RT. Cells were incubated with anti-DR5 antibody and reacted with a rhodamine-conjugated secondary antibody, followed by further incubation with 10 μg/ml fluorescein isothiocyanate-labeled cholera toxin B (FITC-CTxB) and 1 μg/ml HO for 30 min. Cellular localization of anti-DR5 and rafts was observed under a laser-scanning confocal microscope (×600; FV1000; Olympus Optical Co., Tokyo, Japan). Using an argon laser, FITC and rhodamine were excited at 488 nm, and the evoked emission was filtered with a 515 nm (FITC) or 515–605 nm (rhodamine) band-pass filter. HO was excited at 405 nm with a diode laser and emission was filtered at 400–450 nm.

In vivo tumor xenograft study

Six-week-old BALB/c nu/nu athymic mice were purchased from Orient Bio (Seoul, Korea). Animal experiments were performed in accordance with institutional guidelines, and the study was approved by the Ethics Committee of the National Cancer Center. SNU601 cells (5×10^6) were implanted subcutaneously into the thigh of mice, and UDCA (40 and 120 mg/kg) was injected into the peritoneal space once a day (6 days/week). As a control, 0.2 ml of saline was injected. Each group consisted of ten mice. Using a caliper, tumor growth was monitored daily by measurement of two perpendicular tumor diameters, and tumor volume was calculated according to a formula: (width^2 × length)/2. At the end of the study, tumors, together with liver and kidney tissues, were resected from mice, and subjected to histopathological examination and it was confirmed that normal liver and kidney tissues were not damaged in mice treated with UDCA. Tumors were fixed, sectioned onto glass slides and subjected to immunohistochemistry for DR5. Counter staining was performed with hematoxylin. Immunostaining intensity = (percentage of tumor section scored as 1) × 1+(percentage of tumor section scored as 2) × 2+(percentage of tumor section scored as 3) ×3.

Statistical analysis

All numerical data are reported as mean ± standard error. All data represent the results of at least three independent experiments. Groups were compared using Student's *t*-test.

Results

UDCA induces apoptosis, but not necrosis, in GC cells

To evaluate the antitumor efficacy of UDCA in GCs, the effects of UDCA on cell viability and cell death mode were examined in four human GC lines, SNU601, SNU638, SNU1 and SNU216, and compared with those of deoxycholic acid (DCA), a tumor-promoting hydrophobic bile acid. These cell lines harbor highly malignant features due to various genetic alterations in p53, p16, K-ras, TGF-βRII and β-catenin (19). Both UDCA and DCA decreased cell viability in these cell lines in a dose-dependent manner (Figure 1A). However, UDCA induced mostly apoptosis without necrotic features, but DCA triggered tumor-promoting necrosis as well as

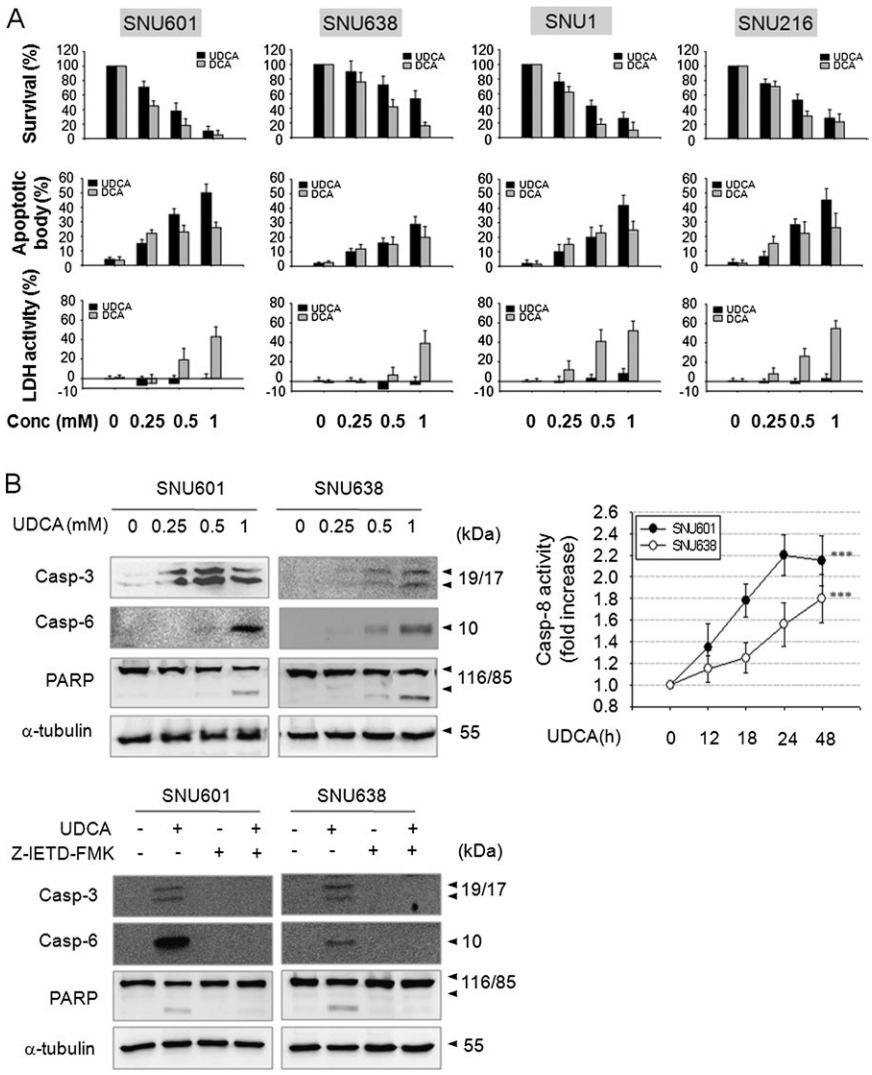

Fig. 1. UDCA suppresses cell viability by inducing apoptotic death in GC cells. (**A**) Cells were exposed to the indicated concentrations of UDCA or DCA for 24 h. Survival, apoptotic nuclei and necrosis were measured by MTT assay, rates of apoptotic body formation and LDH release, respectively. (**B**) Cells were treated with 0.25, 0.5 or 1 mM UDCA (top-left) or 1 mM UDCA with or without 10 μM z-IETD-FMK (bottom), and total proteins were analyzed by immunoblotting for active caspase-3, active caspase-6, PARP and α-tubulin. Caspase-8 activity was measured after treatment with 1 mM UDCA for the indicated times in SNU601 (closed circles) and SNU638 (open circles) cells (right). $^{***}P < 0.001$.

apoptosis, as evidenced by apoptotic body formation and LDH release (Figure 1A). Absence of necrosis in UDCA-induced cell death was confirmed by no significant propidium iodide staining in nucleus (data not shown). In addition, UDCA significantly suppressed the colony-forming ability of these cancer cells (supplementary Figure S1 is available at *Carcinogenesis* Online). UDCA-induced apoptosis was completely suppressed by the inhibitors of caspase-6, -3 and -8 as well as by the pan-caspase inhibitor, and, to a lesser extent, by the caspase-9 inhibitor, but not by the inhibitor of caspase-4 (supplementary Figure S2 is available at *Carcinogenesis* Online). Activation of caspase-3, -6 and -8 was also observed by immunoblotting or measurement of caspase activity (Figure 1B, top), indicating a critical role of the caspase-8/3-mediated extrinsic pathway in the UDCA-induced apoptosis. Furthermore, UDCA-triggered cleavage of caspase-3 and -6, and PARP was prevented by caspase-8 inhibitor (Figure 1B, bottom). Caspase-6 is reported to be the main caspase responsible for toxic bile acid-induced apoptosis in liver cells and activates caspase-8 as a part of a feedback loop (20). In our system, however, UDCA-triggered activation of caspase-3 and -6 was completely blocked by the caspase-8 inhibitor (Figure 1B, bottom), and caspase-6 inhibition did not reduce caspase-8 activity (data not shown), placing caspase-8 upstream of caspase-3 and caspase-6 in the apoptotic pathway of GC cells.

UDCA-triggered apoptosis is regulated by DR5

Because caspase-8 is the dominant DR-triggered caspase, we investigated the possible involvement of DRs, such as Fas, DR4 and DR5 in UDCA-induced apoptosis. UDCA induced a significant increase in the messenger RNA level of DR5, but not that of DR4, Fas or TRAIL, as revealed by real-time polymerase chain reaction analysis in both SNU601 and SNU638 cells (Figure 2A, top). Accordingly, the protein level of DR5, but not DR4 or Fas, was remarkably increased in a dose- and time-dependent manner (Figure 2A, mid and bottom). Transfection with siRNA for DR5, but not with control siRNA, resulted in profound suppression of UDCA-induced apoptosis (Figure 2B, top) and clearly diminished cleavage of caspase-3, caspase-6 and PARP as well as activation of caspase-8 (Figure 2B, bottom), indicating that UDCA induces apoptosis through DR5 expression. Knockdown of FADD and RIP1, downstream adapters for DR5, also reduced UDCA-induced caspase-8 activation, and cleavage of caspase-3, caspase-6 and PARP (Figure 2C). These results indicate that UDCA-induced

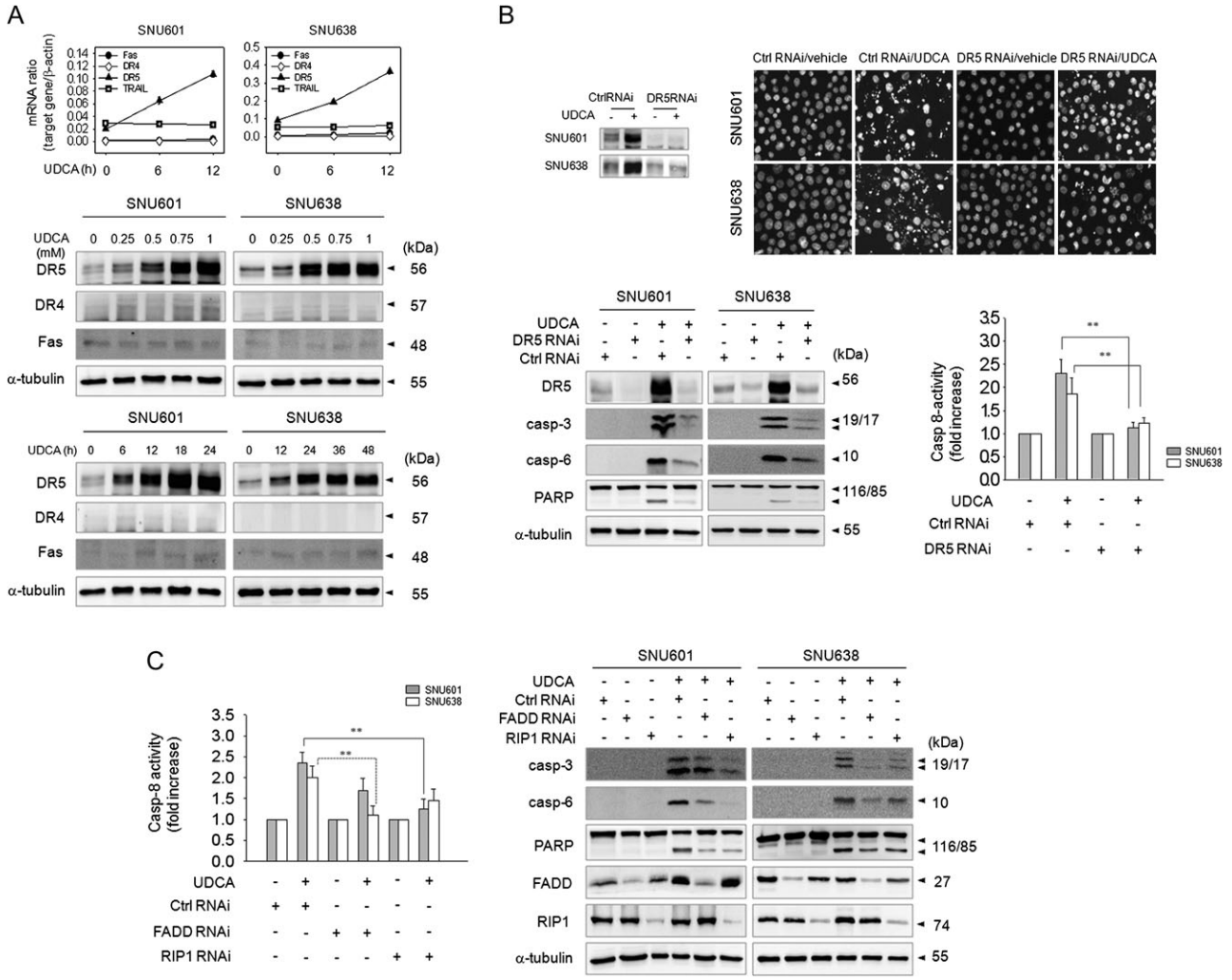

Fig. 2. UDCA-induced apoptosis is mediated by DR5. (**A**) SNU601 and SNU638 cells were exposed to 1 mM UDCA, and messenger RNA levels of Fas, DR4, DR5 and TRAIL were analyzed by real-time PCR (top). Cells treated with various concentrations of UDCA for 24 h or various durations of 1 mM UDCA were analyzed by immunoblotting (bottom). (**B**) Cells transfected with DR5 siRNA or scrambled siRNA (Ctrl RNA interference) were treated with 1 mM UDCA and DR5 interference was confirmed by immunoblotting (top-left) or nuclear images were taken after HO staining using fluorescence microscopy (top-right). Total proteins were subjected to immunoblotting (bottom-left) or analyzed by a caspase-8 activity assay (bottom-right). $^{**}P < 0.005$. (**C**) Cells were transfected with FADD, RIP1 or scrambled siRNA (Ctrl RNA interference) for 24 h and treated with 1 mM UDCA. Total protein extracts were subjected to caspase-8 activity assay (left) or immunoblotting (right). $^{**}P < 0.005$.

apoptosis is mediated by DR5, which signals activation of caspase-8 through RIP1 or FADD.

UDCA-induced apoptosis is regulated by lipid rafts

Several reports have suggested a role for UDCA as a membrane stabilizer and ligand-independent DR activation is often linked to membrane raft aggregation (21–24); therefore, we questioned if UDCA triggers DR5 activation through alterations of membrane events, such as lipid raft formation. In fact, UDCA increased lipid raft structure, as visualized by confocal microscopy with FITC-CTxB as a raft marker and DR5 co-localized with lipid rafts, and methyl-beta-cyclodextrin (MBCD), a lipid raft-disrupting agent blocked these events (Figure 3A). To further define DR5 localization into lipid rafts, we separated rafts from the disordered membrane environment using a discontinuous sucrose density gradient. A total of 12 fractions of 1 ml each were collected and analyzed biochemically for their cholesterol, protein contents and the presence of raft marker caveolin-1. In SNU601 and SNU638 cells, fractions 4–5 and fractions 3–4 were identified as lipid rafts, respectively. In the presence of UDCA, DR5 and DISC proteins were detected in the raft region (Figure 3B). As DRs are required to localize into lipid rafts for their efficient activation, we assumed that lipid raft disruption may prevent UDCA-induced apoptosis. In fact, MBCD completely blocked apoptosis (Figure 3C, top) and replenishment of cholesterol restored apoptosis (supplementary Figure S3 is available at *Carcinogenesis* Online), confirming an essential role of lipid rafts in UDCA-induced apoptosis. In addition, unexpectedly, MBCD clearly prevented DR5 accumulation, as well as cleavage of caspase-3, -6 and PARP in immunoblot assays using total protein extracts (Figure 3C, bottom). Therefore, lipid rafts appeared to play a critical role in activation of the signal that regulates DR5 expression, not only DR5 relocalization.

ROS is involved in UDCA-induced raft-dependent DR5 upregulation

In many cases, lipid raft formation is closely associated with ROS signal. ROS is implicated in lipid raft aggregation and lipid rafts also control ROS generation through reduced nicotinamide adenine dinucleotide phosphate (NADPH) oxidase (25–28). In addition, oxidative stress by chemosensitizer or chemopreventive agents, such as LY303511 and curcumin has been implicated in DR5 upregulation (29–31). These results prompted us to examine whether ROS is involved in UDCA-induced raft-dependent DR5 upregulation. We found that UDCA highly augmented ROS production, as revealed

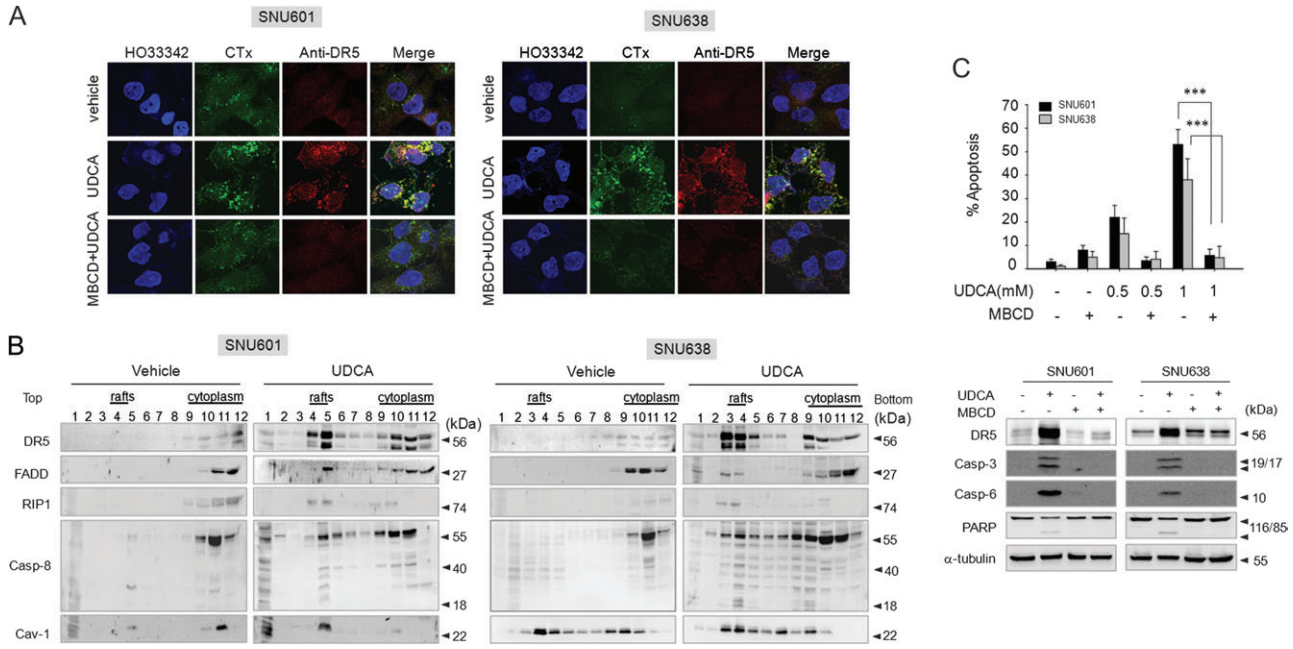

Fig. 3. UDCA-induced apoptosis is regulated by lipid rafts. (**A**) Cells were treated with vehicle, 1 mM UDCA or 1mM MBCD + 1 mM UDCA for 12 h. After fixation, cells were stained with anti-DR5/FITC-CTxB/HO and observed under a confocal microscope. (**B**) Cells were treated with 1 mM UDCA for 24 h and rafts were separated using sucrose-gradient centrifugation, and a total of 12 fractions of 1 ml each were then collected and analyzed by immunoblotting using antibodies against DR5, FADD, RIP1, caspase-8 and caveolin-1. (**C**) Cells treated with UDCA in the absence or presence of 1 mM MBCD were analyzed for apoptosis by HO staining and apoptotic nuclei were counted under a fluorescence microscope (top) or subjected to immunoblotting (bottom). $^{***}P < 0.001$.

by 2′,7′-dicloroﬂuorescin ﬂuorescence (Figure 4A, top). We examined the effects of several antioxidants on UDCA-induced apoptosis and DR5 induction; the concentrations of the antioxidants in the study were chosen within commonly used ranges, and the activity of catalase was confirmed in our previous study (18). The general ROS scavenger, N-acetyl-L-cysteine (NAC), almost completely blocked apoptosis and DR5 induction and the superoxide anion scavenger BHA and the lipid peroxidation inhibitor trolox showed a lesser but considerable effect; however, catalase had no effect (Figure 4A, mid and bottom). Based on these results, superoxide anion or superoxide radicals, but not hydrogen peroxide, appears to be major ROS-mediating DR5 elevation and apoptosis. Next, we examined the possible involvement of Rac1-dependent NADPH oxidase activation in UDCA-induced DR5 induction since NADPH oxidase is implicated in raft-dependent ROS production (28). The NADPH oxidase inhibitor, diphenylene iodonium reduced UDCA-induced ROS generation (data not shown) and showed a considerable inhibitory effect on apoptosis and DR5 induction (Figure 4A). In addition, UDCA activated NADPH oxidase which was reduced by MBCD, and knockdown of Rac1 decreased expression of DR5 (Figure 4B); hence, activation of NADPH oxidase may be one of the possible mechanisms of ROS generation inducing DR5 expression which is controlled by lipid rafts. In agreement with this, MBCD significantly inhibited ROS production in response to UDCA (Figure 4C). However, NAC also considerably suppressed the raft formation (Figure 4D). Therefore, UDCA-induced DR5 upregulation is mediated by both ROS generation and raft formation, and these two factors seemed to amplify each other for their proper activation.

UDCA-induced DR5 upregulation is mediated by PKCδ

As certain isotypes of PKC are involved in DR5 expression by various antitumor agents, such as quercetin or melatonin in different cells (32–34), we investigated whether PKC is associated with UDCA-triggered DR5 induction. First, we examined if UDCA activates PKC isoforms. Since PKC isoforms require negatively charged phospholipids for their optimal activity, translocation of PKC into the plasma membrane is one of the manifestations of its activation. Following UDCA treatment, increase of PKCδ, but not PKCα, PKCε or PKCθ in the membranous fraction was detected at 2–4 h and 4–8 h in SNU601 and SNU638 cells, respectively (Figure 5A). Moreover, the PKCδ inhibitor, rottlerin, but not other PKC inhibitors, GO6979 or GF109203X, significantly reduced DR5 upregulation as well as caspase-3 and caspase-6 cleavage (Figure 5B, left). Knockdown of PKCδ also resulted in a similar suppressive effect on DR5 induction and caspase-3 and -6 cleavages (Figure 5B, right). Suppression of PKCδ by rottlerin or siRNA also reduced UDCA-induced apoptosis (data not shown). Furthermore, PKCδ translocation was inhibited by ROS suppressors NAC, BHA and diphenylene iodonium as well as MBCD (Figure 5C). Altogether, PKCδ appeared to mediate UDCA-triggered DR5 induction through lipid raft/ROS-dependent activation.

In vivo study of the antitumor effects of UDCA on xenografts

We explored the *in vivo* antitumor activity of UDCA in nude mice-bearing SNU601 xenografts by serial measurement of tumor volumes and tissue analysis. A high dose (120 mg/kg) and a low dose (40 mg/kg) of UDCA and vehicle were injected intraperitoneally daily (six times a week) into nude mice ($n = 10$ each) bearing established SNU601 tumor xenografts. At 33 days after tumor inoculation, tumor growth was inhibited by 33.4 and 13.2%, in the high- and low-dose treatment groups, respectively, relative to control mice injected with saline (Figure 6A). A significant reduction in tumor volume was observed in the high dose group ($P < 0.05$) but not in the low-dose group ($P > 0.05$). Since UDCA-induced apoptosis was mediated by DR5 expression at the cellular level, immunohistochemical analysis was performed to assess DR5 expression level in the tumors after killing the mice. DR5 was detected at low levels in the tumor tissues of the vehicle or the low dose treated group and increased levels of DR5 were detected in those of the high dose treated group, specifically around cell death regions ($P < 0.05$), indicating that UDCA may induce cell death through DR5 expression in the xenografts (Figure 6B).

Discussion

In the present study, we report on a novel activity of UDCA as a powerful apoptotic inducer in GC cells. Although the anti-apoptotic role of UDCA in hepatocytes has been widely known, recent evidence has

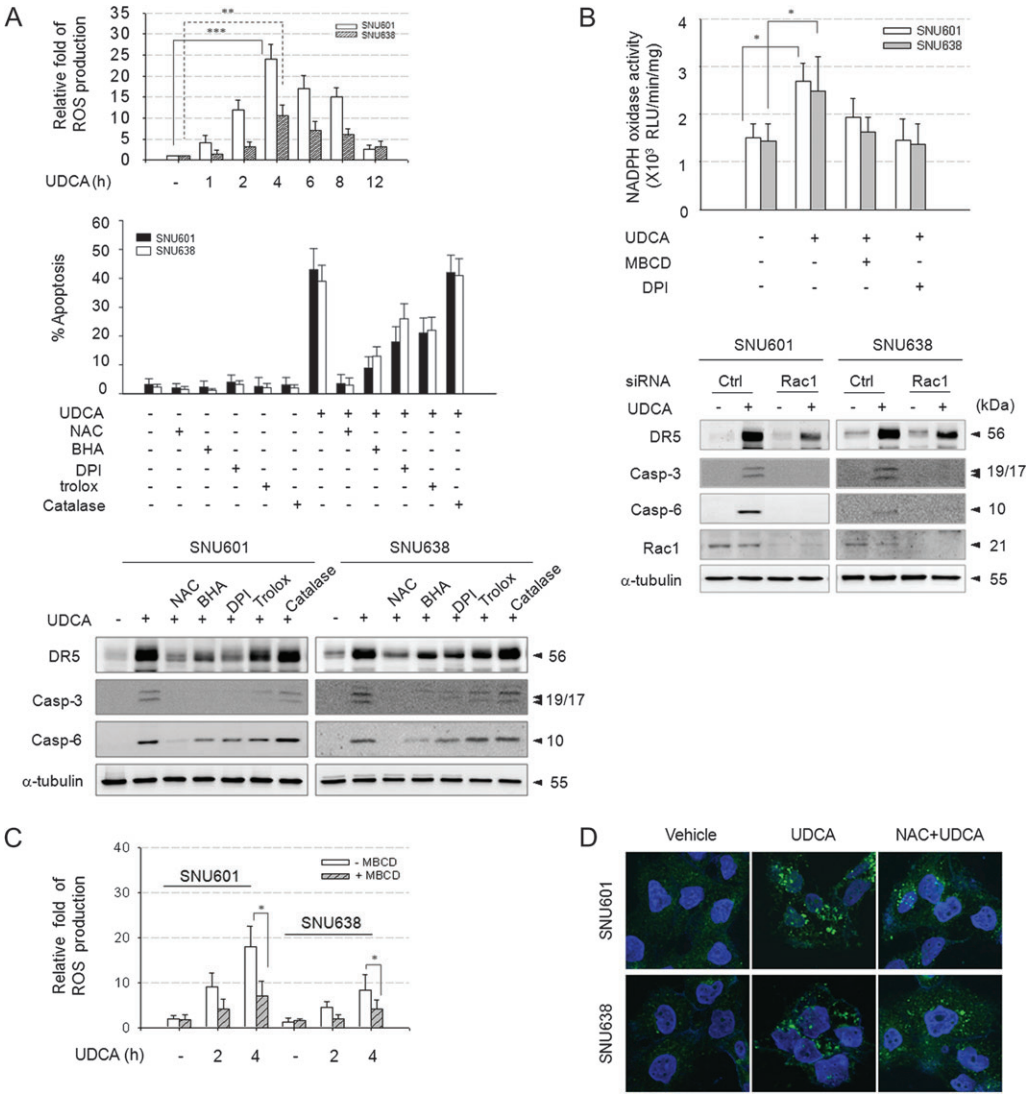

Fig. 4. UDCA-triggered DR5 induction is mediated by ROS generation. (**A**) Intracellular ROS level was measured by 50 μM DCFH-DA after incubation with UDCA for the indicated times using a fluorocounter (top), and cells pre-treated with 10 mM NAC, 50 μM BHA, 1 μM diphenylene iodonium, 100 μM trolox or 1000 U catalase were incubated with UDCA and analyzed for apoptosis by HO staining and apoptotic nuclei were counted under a fluorescence microscope (mid) or by immunoblotting (bottom). $^{**}P < 0.005$, $^{***}P < 0.001$ (**B**) Cells treated with 1 m UDCA, 1 mM MBCD plus 1 mM UDCA or 1 μM diphenylene iodonium plus 1 mM UDCA for 8 h were subjected for the NADPH oxidase activity assay (top), and cells transfected with scrambled siRNA or Rac1 siRNA were incubated with 1 mM UDCA and analyzed by immunoblotting (bottom). $^{*}P < 0.01$. (**C**) Cells treated with 1 mM UDCA alone or co-treated with 1 mM MBCD were analyzed for ROS production using DCFH-DA at 2 and 4 h after UDCA treatment. $^{*}P < 0.01$ (**D**) Cells exposed to vehicle, 1 mM UDCA alone or 10 mM NAC plus UDCA were stained with FITC-CTxB and observed under a confocal microscope.

revealed the potential of UDCA as a pro-apoptotic inducer under certain conditions (35–37). For example, UDCA enhances CPT-11-induced apoptosis in colon cancer cells and increases oxaliplatin-induced apoptosis by modulation of the death mode in HepG2 cells (35,37). We found that DR5 is a main effecter responsible for UDCA-induced apoptosis of GCs (Figure 2); however, we do not exclude the possible involvement of other DRs. UDCA increased the protein level of DR5 through transcriptional regulation and also activated recruitment of DR5 into lipid rafts (Figures 2 and 3). Upon DR5 activation, FADD and caspase-8 mediate apoptotic signals by formation of DISCs in lipid rafts of the plasma membrane (38). In accordance with this observation, FADD, RIP1 and caspase-8 translocated into the raft region by UDCA (Figure 3B), and knockdown of FADD or RIP1 strongly suppressed UDCA-triggered apoptosis (Figure 2C). However, the level of ligand TRAIL was not increased by UDCA (Figure 2A, top); thus, UDCA-induced DR5 activation may be regulated in a ligand-independent fashion. Recently, TRAIL and its receptors have been regarded as a highly promising endogenous antitumor system, and research into various immuno- and chemotherapeutic approaches to utilization of this pathway for efficient tumor cell killing is ongoing (39). Nevertheless, TRAIL resistance has been observed in various cancer cells in which the DR pathway is not efficiently activated. Therefore, a combination of TRAIL with a tumor-sensitizing agent, such as zerumbone or quercetin, has been suggested as a strategy to overcome this limitation, since these sensitizers induce highly enhanced activation of the DR pathway by elevation of DR5 expression (31,34,40). In this regard, the property of UDCA for induction of both DR5 expression and activation/localization into rafts is suggestive of its promise as a powerful tumor sensitizer.

Here, our results highlighted a central role(s) for lipid rafts in UDCA-induced apoptosis. Prevention of raft formation by MBCD significantly suppressed ROS production and resulted in nearly profound blockage of PKCδ activation, DR5 expression and relocalization, thereby completely protecting cells from apoptosis. Significant evidence has demonstrated the importance of lipid rafts in DR-induced apoptosis, and DRs are believed to be efficiently clustered on

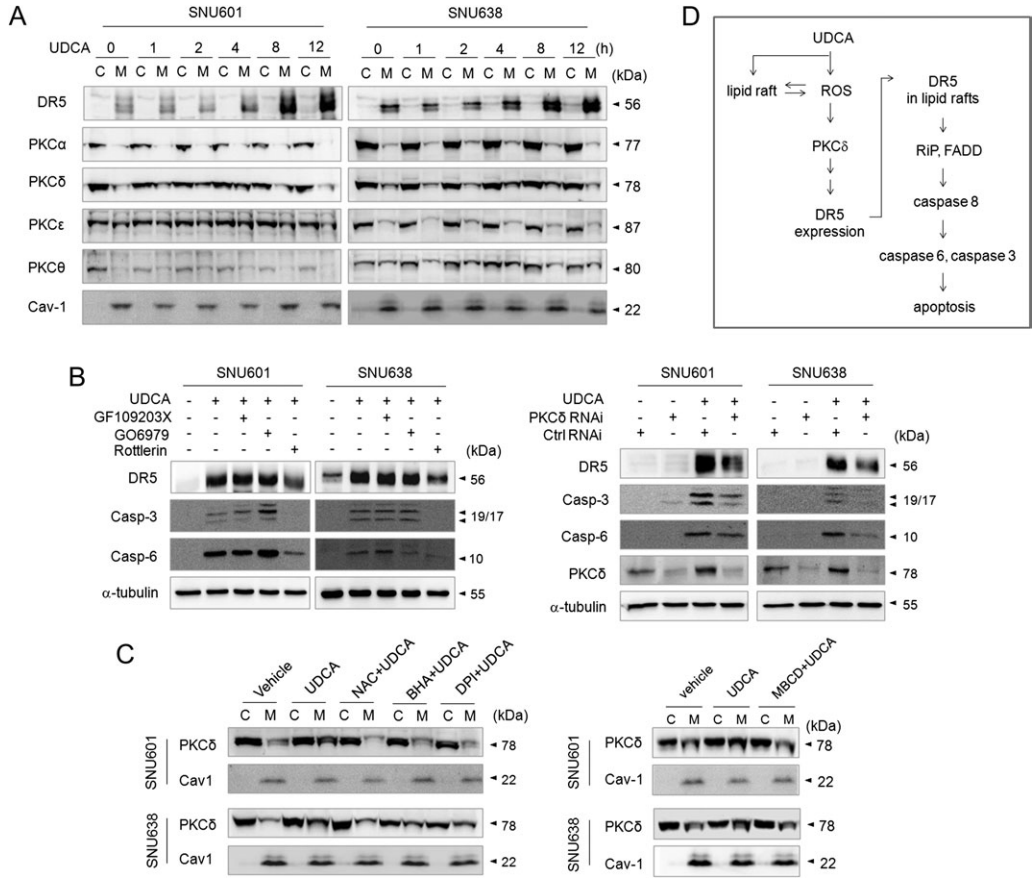

Fig. 5. UDCA-induced apoptosis and DR5 expression are regulated by PKCδ. (**A**) Cells exposed to 1 mM UDCA for the indicated times were separated into cytosolic and membrane fractions and then analyzed by immunoblotting. (**B**) Cells pre-exposed to 1 μM GO6979, 1 μM GF109203X and/or 5 μM rottlerin (left) or transfected with scrambled siRNA or PKCδ siRNA (right) were incubated with 1 mM UDCA and analyzed by immunoblotting. (**C**) Cells exposed to vehicle, 1 mM UDCA, 10mM NAC plus 1mM UDCA, 50 μM BHA plus 1mM UDCA, 1 μM diphenylene iodonium plus 1mM UDCA or 1 mM MBCD plus 1 mM UDCA were separated into cytosolic and membrane fractions and analyzed by immunoblotting for PKCδ and caveolin-1. (**D**) Model for UDCA-induced apoptosis in GCs.

aggregated lipid rafts for induction of apoptosis (17). Anticancer agents, cisplatin, doxorubicin and the alkylphospholipid induce DR-mediated apoptosis via signaling through lipid raft formation (16,27) and lipid rafts have emerged as an efficient therapeutic target of various cancer cells, including myeloma, lymphoma and hepatoma (41–43). In general, antitumor drug-induced raft formation is responsible for DR relocalization (15,27); however, UDCA-triggered raft formation was linked not only to membrane localization but also DR5 expression, indicating that raft formation by UDCA is a very early event necessary for DR5 expression. In addition, raft aggregation was closely linked with ROS generation, as supported by a number of studies, which suggested that ROS triggers raft formation (27); however, our study also demonstrated that rafts contribute to generation of ROS, probably through activation of NADPH oxidase. UDCA can be incorporated into the plasma membrane in a manner similar to that of cholesterol and plays a role as a membrane stabilizer (21,22), and the membrane-stabilizing ;effect of UDCA is dependent on the membrane cholesterol level (44). These findings imply that UDCA may directly trigger lipid raft formation through physical interaction with the plasma membrane. In this regard, it is possible that UDCA may simultaneously stimulate rafts and ROS generation by acting on the cell membrane, and they positively activate each other's signal. On the other hand, ROS was responsible for induction of apoptosis and DR5 expression, which were completely prevented by NAC; however, the NADPH oxidase inhibitor, diphenylene iodonium or knockdown of Rac1 only partially inhibited UDCA-induced apoptosis and DR5 expression level, implying that other ROS-generating mechanisms are also involved in a UDCA-induced apoptotic pathway. Next, PKCδ was also demonstrated as a mediator of the UDCA signal in GCs and this is the first study showing role of UDCA on PKCδ activation. Previously, UDCA was reported to suppress DCA-induced activation of PKC isozymes in colonic cancer cells, thereby suppressing DCA-induced carcinogenesis (45). However, the effect of UDCA on PKCδ seems to be differently regulated in GCs.

We also examined the effect of UDCA on GCs in an *in vivo* system. In xenograft mice, 120 mg/kg UDCA induced the demise of tumor tissue and a statistically significant ($P < 0.05$) 33.4% reduction in tumor size. In the present study, the role of UDCA was studied at relatively high concentration ranges; however, we found no apparent sign of toxicity in the distinct organs analyzed following necropsy. Recently, other groups have reported that feeding 5 mg/mouse/day UDCA is safe in a mouse model (46). This is approximately equal to 250 mg/kg/day. Thus, the dose used in this study appears to be within a safe range. In addition, 1 mM UDCA did not induce cell death in normal rat gastric cell lines, IEC-6 and IEC-18 (data not shown), and the apoptotic effect of UDCA was less effective in other cancer cells originating from various organs, including HT29, SK-Hep1 and A549 (data not shown); however, all four tested GC cell lines were highly sensitive to UDCA. These results imply a selective pro-apoptotic function of UDCA in GC cells. However, it is not clear what makes GC more sensitive to UDCA. Raft formation is a critical mechanism in UDCA-induced apoptotic signaling; therefore, certain features of lipid membranes, such as different lipid composition or altered contents of raft components, may be involved in the sensitivity of GC. In fact, it has been reported that the phospholipid fatty acid composition is different between malignant and benign human gastric tissue and that cholesterol content in tumor cells is higher than in corresponding normal cells (47–49). Alteration of membrane features may enhance

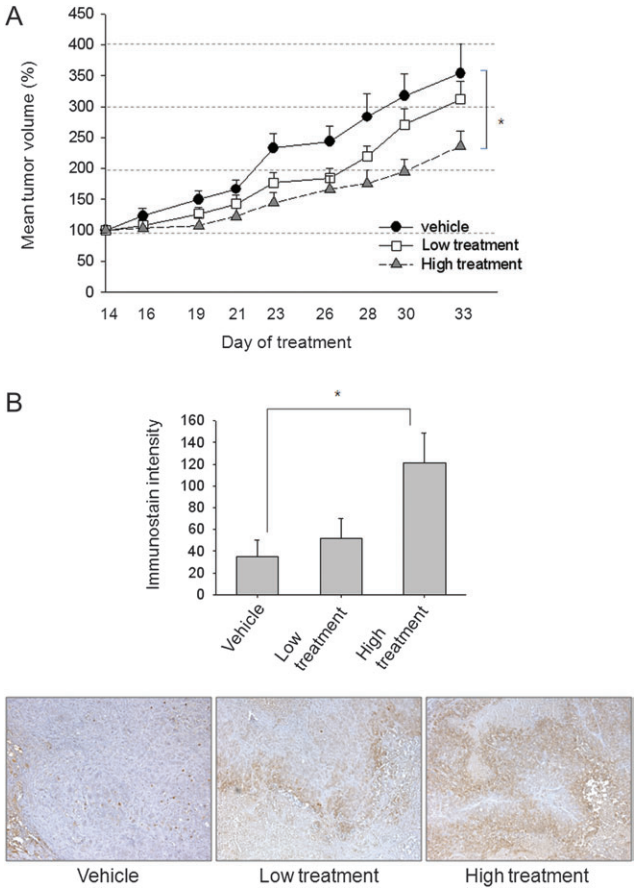

Fig. 6. Antitumor effect of UDCA in gastric cancer xenograft models. (**A**) SNU601 cells were implanted into athymic mice subcutaneously, and mice were injected (intraperitoneally) with vehicle, 40 mg/kg UDCA (low treatment) and 120 mg/kg UDCA (high treatment) once a day and tumor growth was monitored, as described in the Materials and Methods. $^{*}P < 0.01$ (**B**) Tumors from control mice or mice treated with 40 mg/kg UDCA (low treatment) and 120 mg/kg UDCA (high treatment) were harvested, sectioned and analyzed by immunohistochemistry for DR5.

membrane affinity to UDCA or increase UDCA uptake that enables selective tumor targeting, as demonstrated in preferential accumulation of lipid raft-targeting alkyl-lysophosphlipids in the tumor (50). It may also produce changes in membrane fluidity, which may alter the ability of raft formation, and thus, sensitize the ability for recruitment of pro-apoptotic molecules. Although further studies are required in order to clarify the exact mechanism of lipid raft regulation, our study suggests that modulation of lipid raft formation by UDCA may provide a novel therapeutic strategy for treatment and prevention of GC.

Supplementary material

Supplementary Figures S1–S3 can be found at http://carcin.oxfordjournals.org/

Funding

This work was supported by the National Research Foundation of Korea (NRF) grant funded by the Korea government (MEST) through the Research Center for Resistant Cells (R13-2003-009).

Acknowledgements

The authors would like to thank Prof Ho Sung Kang, Department of Molecular Biology, Pusan National University and Prof. Tae-Hyoung Kim, Department of Biochemistry, Chosun University for critical reading and discussion.

References

1. Pisani,P. *et al*. (1999) Estimates of the worldwide mortality from 25 cancers in 1990. *Int. J. Cancer.*, **83**, 18–29.
2. Lordick,F. *et al*. (2010) Cetuximab plus oxaliplatin/leucovorin/5-fluorouracil in first-line metastatic gastric cancer: a phase II study of the Arbeitsgemeinschaft Internistische Onkologie (AIO). *Br. J. Cancer*, **102**, 500–505.
3. Marzioni,M. *et al*. (2006) Ca2+-dependent cytoprotective effects of ursodeoxycholic and tauroursodeoxycholic acid on the biliary epithelium in a rat model of cholestasis and loss of bile ducts. *Am. J. Pathol*, **168**, 398–409.
4. Loddenkemper,C. *et al*. (2006) Prevention of colitis-associated carcinogenesis in a mouse model by diet supplementation with ursodeoxycholic acid. *Int. J. Cancer*, **118**, 2750–2757.
5. Kohno,H. *et al*. (2007) Ursodeoxycholic acid versus sulfasalazine in colitis-related colon carcinogenesis in mice. *Clin. Cancer Res.*, **13**, 2519–2525.
6. Alberts,D.S. *et al*. (2005) Phase III trial of ursodeoxycholic acid to prevent colorectal adenoma recurrence. *J. Natl Cancer Inst.*, **97**, 846–853.
7. Khare,S. *et al*. (2003) Ursodeoxycholic acid inhibits Ras mutations, wild-type Ras activation, and cyclooxygenase-2 expression in colon cancer. *Cancer Res.*, **63**, 3517–3523.
8. Fein,M. *et al*. (2000) Duodenogastric reflux and foregut carcinogenesis: analysis of duodenal juice in a rodent model of cancer. *Carcinogenesis*, **21**, 2079–2084.
9. Rosman,A.S. (1987) Efficacy of UDCA in treating bile reflux gastritis. *Gastroenterology*, **92**, 269.
10. Rock,K.L. *et al*. (2008) The inflammatory response to cell death. *Annu. Rev. Pathol.*, **3**, 99–126.
11. Vakkila,J. *et al*. (2004) Inflammation and necrosis promote tumour growth. *Nat. Rev. Immunol.*, **4**, 641–648.
12. Walczak,H. *et al*. (1997) TRAIL-R2: a novel apoptosis-mediating receptor for TRAIL. *EMBO J.*, **16**, 5386–5397.
13. Walczak,H. *et al*. (1999) Tumoricidal activity of tumor necrosis factor-related apoptosis-inducing ligand *in vivo*. *Nat. Med.*, **5**, 157–163.
14. Medema,J.P. *et al*. (1997) FLICE is activated by association with the CD95 death-inducing signaling complex (DISC). *EMBO J.*, **16**, 2794–2804.
15. Gajate,C. *et al*. (2004) Intracellular triggering of Fas aggregation and recruitment of apoptotic molecules into Fas-enriched rafts in selective tumor cell apoptosis. *J. Exp. Med.*, **200**, 353–365.
16. Gajate,C. *et al*. (2007) Edelfosine and perifosine induce selective apoptosis in multiple myeloma by recruitment of death receptors and downstream signaling molecules into lipid rafts. *Blood*, **109**, 711–719.
17. Lingwood,D. *et al*. (2010) Lipid rafts as a membrane-organizing principle. *Science*, **327**, 46–50.
18. Kim,C.H. *et al*. (2007) Protein kinase C-ERK1/2 signal pathway switches glucose depletion-induced necrosis to apoptosis by regulating superoxide dismutases and suppressing reactive oxygen species production in A549 lung cancer cells. *J. Cell. Physiol.*, **211**, 371–385.
19. Ku,J.L. *et al*. (2005) Biology of SNU cell lines. *Cancer Res. Treat.*, **37**, 1–19.
20. Rust,C. *et al*. (2009) Bile acid-induced apoptosis in hepatocytes is caspase-6-dependent. *J. Biol. Chem.*, **284**, 2908–2916.
21. Guldutuna,S. *et al*. (1997) Ursodeoxycholate stabilizes phospholipid-rich membranes and mimics the effect of cholesterol: investigations on large unilamellar vesicles. *Biochim. Biophys. Acta*, **1326**, 265–274.
22. Guldutuna,S. *et al*. (1993) Molecular aspects of membrane stabilization by ursodeoxycholate [see comment]. *Gastroenterology*, **104**, 1736–1744.
23. Xu,Z.X. *et al*. (2009) Avicin D, a plant triterpenoid, induces cell apoptosis by recruitment of Fas and downstream signaling molecules into lipid rafts. *PLoS One*, **4**, e8532.
24. Muppidi,J.R. *et al*. (2004) Ligand-independent redistribution of Fas (CD95) into lipid rafts mediates clonotypic T cell death. *Nat. Immunol.*, **5**, 182–189.
25. Shin,D.M. *et al*. (2008) Mycobacterium tuberculosis lipoprotein-induced association of TLR2 with protein kinase C zeta in lipid rafts contributes to reactive oxygen species-dependent inflammatory signalling in macrophages. *Cell. Microbiol*, **10**, 1893–1905.
26. Yang,B. *et al*. (2006) Lipid rafts mediate H2O2 prosurvival effects in cultured endothelial cells. *FASEB J.*, **20**, 1501–1503.
27. Lacour,S. *et al*. (2004) Cisplatin-induced CD95 redistribution into membrane lipid rafts of HT29 human colon cancer cells. *Cancer Res.*, **64**, 3593–3598.
28. Schilling,T. *et al*. (2010) Importance of lipid rafts for lysophosphatidylcholine-induced caspase-1 activation and reactive oxygen species generation. *Cell. Immunol.*, **265**, 87–90.

29. Jung,E.M. *et al*. (2005) Curcumin sensitizes tumor necrosis factor-related apoptosis-inducing ligand (TRAIL)-induced apoptosis through reactive oxygen species-mediated upregulation of death receptor 5 (DR5). *Carcinogenesis*, **26**, 1905–1913.
30. Kwon,D. *et al*. (2008) Hydrogen peroxide enhances TRAIL-induced cell death through up-regulation of DR5 in human astrocytic cells. *Biochem. Biophys. Res. Commun.*, **372**, 870–874.
31. Yodkeeree,S. *et al*. (2009) Zerumbone enhances TRAIL-induced apoptosis through the induction of death receptors in human colon cancer cells: evidence for an essential role of reactive oxygen species. *Cancer Res.*, **69**, 6581–6589.
32. Jones,B.A. *et al*. (1997) Bile salt-induced apoptosis of hepatocytes involves activation of protein kinase C. *Am. J. Physiol.*, **272**, G1109–G1115.
33. Rao,Y.P. *et al*. (1997) Activation of protein kinase C alpha and delta by bile acids: correlation with bile acid structure and diacylglycerol formation. *J. Lipid Res.*, **38**, 2446–2454.
34. Song,J.H. *et al*. (2008) ABT-737 induces expression of the death receptor 5 and sensitizes human cancer cells to TRAIL-induced apoptosis. *J. Biol. Chem.*, **283**, 25003–25013.
35. Ikegami,T. *et al*. (2006) Enhancement of DNA topoisomerase I inhibitor-induced apoptosis by ursodeoxycholic acid. *Mol. Cancer Ther.*, **5**, 68–79.
36. Qiao,L. *et al*. (2002) Inhibition of the MAPK and PI3K pathways enhances UDCA-induced apoptosis in primary rodent hepatocytes. *Hepatology*, **35**, 779–789.
37. Lim,S.C. *et al*. (2010) Ursodeoxycholic acid switches oxaliplatin-induced necrosis to apoptosis by inhibiting reactive oxygen species production and activating p53-caspase 8 pathway in HepG2 hepatocellular carcinoma. *Int. J. Cancer*, **126**, 1582–1595.
38. Bodmer,J.L. *et al*. (2000) TRAIL receptor-2 signals apoptosis through FADD and caspase-8. *Nat. Cell Biol.*, **2**, 241–243.
39. Lee,J.Y. *et al*. (2007) The NO TRAIL to YES TRAIL in cancer therapy (review). *Int. J. Oncol.*, **31**, 685–691.
40. Chen,W. *et al*. (2007) Induction of death receptor 5 and suppression of survivin contribute to sensitization of TRAIL-induced cytotoxicity by quercetin in non-small cell lung cancer cells. *Carcinogenesis*, **28**, 2114–2121.
41. Mollinedo,F. *et al*. (2010) Lipid raft-targeted therapy in multiple myeloma. *Oncogene*, **29**, 3748–3757.
42. van der Luit,A.H. *et al*. (2007) A new class of anticancer alkylphospholipids uses lipid rafts as membrane gateways to induce apoptosis in lymphoma cells. *Mol. Cancer Ther.*, **6**, 2337–2345.
43. Jimenez-Lopez,J.M. *et al*. (2010) Alterations in the homeostasis of phospholipids and cholesterol by antitumor alkylphospholipids. *Lipids Health Dis.*, **9**, 33.
44. Zhou,Y. *et al*. (2009) The role of membrane cholesterol in determining bile acid cytotoxicity and cytoprotection of ursodeoxycholic acid. *Biochim. Biophys. Acta*, **1788**, 507–513.
45. Shah,S.A. *et al*. (2005) Ursodeoxycholic acid inhibits translocation of protein kinase C in human colonic cancer cell lines. *Eur. J. Cancer*, **41**, 2160–2169.
46. Thao,T.D. *et al*. (2008) Antibacterial and anti-atrophic effects of a highly soluble, acid stable UDCA formula in *Helicobacter pylori*-induced gastritis. *Biochem. Pharmacol.*, **75**, 2135–2146.
47. Dessi,S. *et al*. (1994) Cholesterol content in tumor tissues is inversely associated with high-density lipoprotein cholesterol in serum in patients with gastrointestinal cancer. *Cancer*, **73**, 253–258.
48. Freeman,M.R. *et al*. (2004) Cholesterol and prostate cancer. *J. Cell. Biochem.*, **91**, 54–69.
49. Nakazawa,I. *et al*. (1977) Lipid-chemical features of human gastric cancerous, polypous and ulcerative tissues. *Tohoku J. Exp. Med.*, **123**, 365–370.
50. Estella-Hermoso de Mendoza,A. *et al*. (2009) Antitumor alkyl ether lipid edelfosine: tissue distribution and pharmacokinetic behavior in healthy and tumor-bearing immunosuppressed mice. *Clin. Cancer Res.*, **15**, 858–864.

Received September 13, 2010; revised February 13, 2011; accepted February 18, 2011